IEEE Access
Multidisciplinary | Rapid Review | Open Access Journal

Received 28 November 2022, accepted 11 December 2022, date of publication 15 December 2022,
date of current version 20 December 2022.

Digital Object Identifier 10.1109/ACCESS.2022.3229586

RESEARCH ARTICLE

Fast Detection of Weak Arc Faults Based on Progressive Singular-Value-Decomposition and Empirical Analyses

YU-LONG SHEN[1] AND ZHIHONG XU[2,3], (Member, IEEE)
[1]Fujian Yongfu Lvneng Technology Company Ltd., Fuzhou 350108, China
[2]College of Electrical Engineering and Automation, Fuzhou University, Fuzhou 350108, China
[3]Engineering Research Center of Smart Distribution Grid Equipment, University of Fujian Province, Fuzhou 350108, China

Corresponding author: Zhihong Xu (fdxzh@fzu.edu.cn)

This work was supported in part by the Fujian Provincial Department of Science and Technology University Industry-University Cooperation Project 2021Y4002, and in part by the Fujian Province Science and Technology Innovation Leading Talent Funding Project 00387024.

ABSTRACT The aim of this study is to provide a fast and reliable approach to detect weak arc faults that do not noticeably distort the bus current, with the minimum possible arc duration required to respond in low-voltage AC systems. Progressive singular-value decomposition is utilized to filter interference components, primarily AC/DC components. Then, the signals are thoroughly decomposed by empirical analytic tools in the time-frequency domain, combined with the fast Fourier transform to enhance feature extraction in the frequency domain. The features are passed to the neural networks, where the networks are trained and validated repetitively by datasets that are randomly selected from the data sampling. The comparison experiments demonstrate the excellent performance of the proposed method under all crucial evaluation criteria of arc-fault detection.

INDEX TERMS Arc discharges, electrical safety, empirical mode decomposition, fault diagnosis, fourier transforms, high intensity discharges, machine learning, neural networks, singular value decomposition, wavelet analysis.

I. INTRODUCTION

An arc fault describes the fire hazard phenomenon of the voltage between electrodes breaking through the insulating medium or an air gap, possibly accompanied by visible luminescence, followed by a discharge that can release up to 20,000 K heat instantly and ignite combustible materials [1]. Case studies have shown that these types of safety threats can be caused by bad or loose connections, aged or damaged electrical systems, faulty switches, outlets and frayed wires [2]. Arc fault is a contributing factor or the main reason for at least 38.71% of the more than 224,000 home electrical fires that occurred in America between 2012 and 2016, which resulted in an economic loss of approximately 6.5 billion dollars and 8,450 civilian injuries or deaths [3]. In the field of electrical safety, arc faults are one of the most serious fault types, and with the continuous increase in electricity consumption and transmission, the discovery of reliable arc-fault detection solutions has become increasingly urgent. However, research on arc-fault detection started in the late 1970s, yet it is still in progress until today [4], and the depth of the subject is revealed by this fact alone. Arc faults can be divided into different categories by the AC or DC systems, the series or parallel connection ways of the circuit, the faulted situations, and the strong or weak distortions they inflict on the line current; each category has unique challenges [5]. Previous surveys summarized the extraction domains and approaches of arc-fault features, as well as the detection methodologies for different categories of arc faults [6], [7]. It is clear that arc-fault detection evolves from depending on basic VI features and threshold diagnosis to more up-to-date non-VI features or engineered VI features combined with machine learning (ML) classification [8]. Generally, although the popularity of ML algorithms as tools for integrating features has

The associate editor coordinating the review of this manuscript and approving it for publication was Gerard-Andre Capolino.

been growing rapidly, the features that need to be extracted are still decided empirically by the knowledge of the signals and decomposition of the experimental data. However, some methods even rely on ML algorithms to decide which features to extract [9]. Based on reviews and comparisons of the established methods and current progress in the field, this study attempts to present a perspective of the underlying logic in the development of arc-fault detection.

Arc faults are normally classified by their signal types. This study is about the detection of arc faults in AC systems with low voltage and current magnitudes. In this field, not all arc faults necessarily cause obvious distortions to the bus current signals; sometimes arc-fault current samples do not show apparent differences from normal signals. These arc faults are classified as 'weak arc faults' in this study, and arc faults that cause apparent distortions to the bus current signals are classified as 'strong arc faults'. Strong arcs that bring apparent distortions to the VI characteristics of the circuits were first addressed by earlier works in this field; they contain much more energy than weak arcs, and thus, are much more threatening. However, strong arcs are easy to detect since many aspects of the circuit are considerably influenced, and basic VI features, such as a zero-crossing shoulder current [10] or a bus current amplitude [11], combined with straightforward threshold detection, are effective in many cases. Nevertheless, threshold detection by current amplitudes sometimes fails in a system with frequent current amplitude fluctuations due to load shifts or operational transitions, and zero-crossing characteristics do not exist in DC systems. Therefore, researchers developed methods to detect strong arcs by the derivative of the current amplitude [12] and fast Fourier transform (FFT) coefficients [13]. Despite the four references listed, they represent long-lasting and widely applied industrial arc-fault detection methods. These methods do not work in the detection of weak arc faults that have similar VI features as normal signals, but they can be easily realized with the lowest costs. Weak arc faults are hard to detect and are less dangerous, but the discharge still releases enough energy to ignite combustibles. Moreover, they continuously inflict harm to the circuits, which causes serious deterioration in the long run; hence, the detection of weak arc faults cannot be neglected.

Since the VI features of weak arc faults are not obvious, with the masking effects of other components of the bus current, detecting weak arc faults by VI features is much more difficult than strong arc faults. To resolve this problem, researchers turned to non-VI features of arc faults. The three most common non-VI features used for arc fault detection are arc flash, magnetic coupling and electromagnetic radiation (EMR). A method that applies general regression neural networks (GRNNs) to detect arc faults by the influence of arc flash on the light spectrum was proposed in [14]. Bao and Jiang proposed a series of methods to detect arc faults by magnetic coupling [15], [16], [17], which required retrofitting the circuits by passing the live line and the neutral line through the current transformer to obtain high-frequency oscillating pulses. The detection methodologies were developed from multiple thresholds of feature values [15] to higher order cumulants [16] and singular values of the extracted features [17], which shows the increasing emphasis on feature engineering. The EMRs of arc faults have been studied for years, and some relevant detection methods are presented in [18], [19], [20], and [21]. From these previous studies, it is clear that when an arc fault occurs, it transmits electromagnetic radiation, and this fact can be used to diagnose arc faults. The EMR-based detection methods evolved from classification by empirically decided thresholds [18], [19] to dynamic thresholds, such as, for example, combining the structural similarity index matrix (SSIM) with a wide band of spectrograms [20] or correlations in characteristic frequencies of radiation [21]. Without the interference of other components brought upon VI characteristics, the non-VI arc-fault features can be more deterministic, and thus, combined with VI features, the detection accuracy is improved. However, to incorporate non-VI features, extra equipment is inevitable, and sometimes the equipment can be quite expensive. In addition, detection by non-VI features usually has the problem of a severely limited detection range compared to detection by VI features [14], [18], [19], [20], [21]. The methods proposed in [15], [16], and [17] do not necessarily have the downside of a limited detection range, but they require renovation of the live line and the neutral line to function, which makes them not applicable in most scenarios without adaptive modifications, but they may still be suitable as part of the integrated electrical safety design of a residential building [17].

With the aim of successfully detecting both strong and weak arc faults without being bound by extra conditions of non-VI feature extraction, detecting arc faults by more sophisticated VI feature engineering or classification methodology has been trending. A method that combines multiple line current features and multiple thresholds was suggested in [22]; if one aspect is not enough to describe arc faults, then more features and thresholds are added. Absolute feature value thresholds may not be sufficiently adaptable; thus, detection based on thresholds of calculated probabilities was introduced in [23] and [24]. The STD of a certain eigenvector was extracted from the PCA matrix of adjacent current data windows in [23], and sparse representation indices of FFT values are the features extracted for [24]. Similar to the probability threshold, the threshold proportional to feature values can protect the adaptiveness of the detection, as well. A method that extracts the current drop and RMS of DWT coefficients and then makes diagnoses by a dynamic threshold proportional to feature values was presented in [25]. Detection by multiple thresholds of the STD of the moving average current and FFT amplitudes [26] or voltage SNR [27] has also been verified. ML classification as the integrational tool to conduct final diagnosis for each sample is becoming increasingly dominant in the field of arc-fault research for three major reasons: the day-by-day development of ML algorithms, the ever-improving computational power, and the increasingly complicated feature extraction. Telford et al.

designed an inspirational method that utilizes trained hidden Markov models to arrange samples into three classes, normal, normal transitional, and arc-fault, instead of the conventional dichotomy of normal and arc-fault states by DWT coefficients [28]. In this way, the arc-fault signals that are difficult to identify are assigned to the class between normal and arc-fault, which enables further operations. Another method using the ensemble machine learning (EML) algorithm to diagnose arc faults by multiple time-domain current features selected by exhaustive search of the optimal solution was also suggested [29]. Since ML algorithms are good at discovering hidden patterns from heuristic features, combining feature extraction by trial-and-error with ML classification performs rather well in many cases.

Empirical mode decomposition (EMD) is currently one of the popular choices for VI feature extraction and is considered to have more adaptability and less information overlap than traditional frequency or time-frequency analytic tools, such as FFT or wavelet transform (WT), as it decomposes a signal by the layer-by-layer IMF numbers of the same time-frequency scale with the signal itself instead of relying on the compression and stretch of a predetermined base FFT or wavelet function. However, it does not calculate energy indices of frequency bands to directly reflect the composition of the original signal in the frequency domain or extract wavelet coefficients of components at different time-frequency scales, which can be further processed, so EMD is not a replacement of FFT or WT. Some newest detection methods are based on EMD and its variations; one example is to detect arc faults by modified variational mode decomposition (VMD) and a support vector machine (SVM) fused with particle swarm optimization (PSO) [30]. Another interesting EMD-based method proposed in [31] directly passes the intrinsic mode function (IMF) numbers obtained by applying EMD on the original signal to the SVM algorithm, where the parameters are adjusted by a genetic algorithm (GA). In contrast to the traditional gradient descent-based approaches with convergence proven by mathematical theorems, optimizing the parameters of one ML tool by another ML tool is an uncommon black-box approach. A statistically better solution is possible, but optimality is not guaranteed; nevertheless, the functionality of the method is supported by experiments. ML networks trained by heuristic features are becoming dominant in many scientific fields because contemporary computational power is more than sufficient to support abundant samples and repetitive calculations, which makes no difference to deterministic methods but is decisively advantageous for adaptive methods; from a result-oriented perspective, as long as the performances of ML classification are satisfactory, it is a practically reliable methodology. The summary of the above research comparison is presented in Table 1.

Motivated by the necessity of detecting arc faults by bus current signals while the load conditions and current amplitudes change frequently in low voltage AC systems, this research proposes a trustable method that detects arc faults from information contained in just one AC current cycle. The proposed method incorporates the progressive singular value decomposition (PSVD) introduced in [32] as the denoised filter; then, it analyzes the signals by the empirical wavelet transform (EWT) and EMD to extract the features of each IMF sequence layer-by-layer in the time-frequency domain, enhanced by the fast Fourier transform (FFT) to extract energy indices of frequency bands in the frequency domain. After feature extraction, backpropagation neural networks (BPNN) are trained by the features. To avoid overfitting, the data are assigned to the training set, verifying set and testing set in a completely random manner, with 80% of the data used to train the neural networks (NNs), 10% of the data used to verify the training results and the remaining 10% of the data used to conduct experiments and comparisons. The choices of the PSVD, EWT, EMD and FFT are based on the aim for an arc-fault detection method that is sufficiently accurate (over 95%) and also as fast as possible. The experimental result of 96.12% accuracy and 0.034 s average detection time on a laptop with an Intel i7-7700HQ CPU and 16 GB of RAM shows that the proposed PSVDEA-NN method is more satisfactory than the methods selected for comparison.

This study tackles the problem of detecting weak arc faults that cannot be detected by overcurrent protection because they do not cause apparent magnitude changes on the bus current, which is a blind spot for previous researches, by an original design of the PSVD filter, a new combination of multiple fast feature extraction tools in time and frequency domains, and a modified application of the NN to conduct diagnoses by integration of features. The test results illustrate the practicality of the proposed method.

II. DESIGN OF THE PROPOSED METHOD

A. EXPERIMENTAL PLATFORM AND BUS CURRENT SAMPLING

The experimental platform displayed in Fig. 1 is constructed according to UL 1699-2008 [32], an American standard for arc-fault circuit interrupters (AFCIs), and GB/T 31146-2014 [33], a Chinese standard for arc-fault detection devices (AFDDs). The experimental platform is identical to the depiction in Fig. 1 in [34]. Two arc generators are alternatively used: a rod-pulling arc generator to simulate series arc faults caused by bad connections and a carbonized-path arc generator to simulate parallel arc faults caused by carbonized paths between damaged wires.

Experimental data are collected from the bus current with a sampling frequency of 100 kHz by a PCIE1816H high-speed sampling card. The PCIE1816H high-speed sampling card is capable of a 1 MHz sampling frequency. However, a 100 kHz sampling frequency is far more practical for industrial applications in regard to cost; an economic AD7606 sampling chip is a common choice to realize 100 kHz sampling frequency for commercial AFDDs. The step motor operates two terminals (rods) of the rod-pulling arc generator to move away from each other at a fixed speed of 0.015 mm/s to

TABLE 1. Structural analysis and comparison of previously published arc-fault detection methods.

Source(s) of the Features	Detection Methodology	Aim of the Design	Limitation(s)
Basic Voltage-current (VI) features: Zero crossing distortions (voltage or current) [10]; Bus current amplitude [11]; Derivative of current amplitude [12]; Energy variations of frequency components (FFT indices) [13]	Threshold detection of unprocessed feature values	Detect strong AC arc faults that distort bus current remarkably	Not useful in detection DC arc faults (zero crossing distortions based methods); Not applicable in detecting weak arc faults that have similar VI features as normal signals
Combination of VI features and non-VI features: Arc flash [14]; Magnetic field coupling [15]-[17]; EMR [18]-[21]	ML classification: GRNN [14]; Threshold detection: Single threshold [18], [19]; Multiple thresholds [15]; Higher order cumulants [16]; SVD values [17]; SSIM and wide band of spectrograms [20]; Frequencies of radiations [21]	Detect arc faults more accurately by deterministic non-VI arc features	Extra equipment; Limited detection range [13], [17]-[20]; Necessary retrofit of circuits [14]-[16]
Engineering VI features: multiple line current-voltage features [22]; STD of certain eigenvector from PCA matrix of adjacent sampling windows [23]; Sparse representation of FFT values [24]; Current drop and RMS of DWT coefficients [25]; STD of moving average current and FFT amplitudes [26]; Voltage SNR [27]; DWT coefficients [28]; Selected time-domain current features [29]; Modified VMD values [30]; EMD extracted features [31]	ML classification: Trained Hidden Markov Models for normal, arc-fault and normal-transient states [28]; Ensemble machine learning [29]; PSO modified SVM [30]; GA-SVM [31]; Threshold detection: Multiple thresholds [22], [26], [27]; Proportional dynamic thresholds [25]; Probability threshold calculated from features and test results [23], [24]	Enhance detection accuracy by engineering VI features to magnify the differences between arc-fault and normal signals, as well as increasing the amount of VI features if it helps better improving the classification	The diagnosis is extensively customized, which brings the risk of overfitting; The detection speed is not guaranteed due to comparatively sophisticated feature engineering

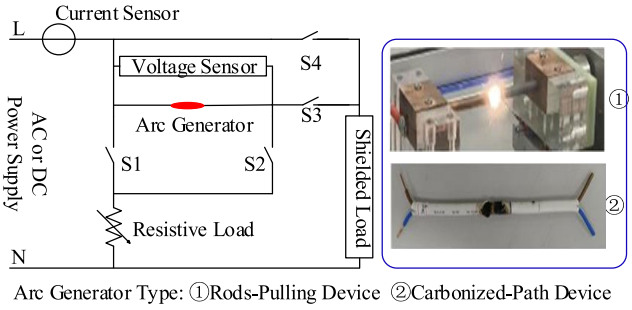

FIGURE 1. Schematic diagram and circuit layout of the experimental platform.

0.03 mm/s for experiments with a current level below 10 A to prolong the stable period of the weak arc fault. For experiments with a current level above 10 A, the speed can be adjusted up to 0.5 mm/s to avoid over-energizing the arc so that the excessively dispersed heat may cause the rods to melt. As the ionization of the air gap progresses and approaches completion, the arc becomes more stable until it breaks when the consistently growing distance between the two rods is too large for this arc to maintain itself with the energy stored. The random nature of the arc makes it difficult to generalize the maximum distance between two rods for arc sustainment in any experiment, but from the experiments of this research, the arcs with the current level below 10 A could not be sustained when the distance was larger than 5 mm. The frequency of the AC power source is 50 Hz.

In total, 2,320 data points contain 1,160 weak arc-fault data points and 1,160 normal data points from a wide variety of load settings, including an electronic dimming light, a squirrel-cage induction motor, resistors, a fluorescent light, a hand drill, a halogen lamp, a switching power supply, and a vacuum cleaner mounted in the experimental circuit. In each experiment, with the AC voltage relatively constant, the bus current fluctuates and is primarily decided by the normal operations of the load if the load is a practically functional appliance. The fluctuation of the current amplitudes inflicts negative effects on the detection; thus, the current amplitude normalization (CAN) approach is incorporated, which protects the data from frequent changes in current amplitudes while preserving the correlations and proportions between indices that describe different aspects of the VI information.

$$G'(g_l) = \frac{G(g_l)}{\max\left[G(g_l)\right] - \min\left[G(g_l)\right]}, \quad l = 1, 2 \ldots, L \quad (1)$$

L is the number of data sampling windows, $G\ (g_l)$ denotes each collected signal, and $G'\ (g_l)$ is the resulting normalized signal. The current amplitude normalization in (1) was also applied in [35].

B. PROGRESSIVE SINGULAR VALUE DECOMPOSITION (PSVD) FOR AC/DC COMPONENTS FILTERING

SVD is one of the most popular choices for unwanted component filtering. The traditional approach is to construct a Hankel matrix from the coefficients of the original signal

sequence in the following form [26]:

$$\boldsymbol{A} = \begin{bmatrix} x(1) & x(2) & \cdots & x(n) \\ x(2) & x(3) & \cdots & x(n+1) \\ \vdots & \vdots & \vdots & \vdots \\ x(N-n+1) & x(N-n+2) & \cdots & x(N) \end{bmatrix} \tag{2}$$

N is the length of the collected signal, and x represents signal sequences. The problem is that the traditional combination of the Hankel matrix and SVD is slow. With the stricter request for a shorter detection time, faster execution of the SVD is becoming increasingly important in breaking through the bottleneck in the detection speed. To address this problem, the PSVD that progressively performs SVD on a signal sequence is a new application approach of the SVD proposed in [34]. The PSVD constructs matrix $\boldsymbol{A}$ by the folding-in-half of the signal rather than by the traditional Hankel matrix construction. Each signal sequence $\boldsymbol{p}$ of length N is folded in half and turned into the following matrix of dimensions 2 by (N / 2):

$$\boldsymbol{A} = \begin{bmatrix} p_0(1) & p_0(2) & \ldots & p_0(N/2) \\ p_0(N/2+1) & p_0(N/2+2) & \ldots & p_0(N) \end{bmatrix} \tag{3}$$

The secondary component of $\boldsymbol{A}$ is the targeted component for feature extraction, and the primary component is filtered because it contains the unwanted AC/DC components with the highest energy levels of the entire signal, as shown by Equation (4):

$$\boldsymbol{A}' = \begin{bmatrix} 0 & 0 & \ldots & 0 \\ p_0(N/2+1) & p_0(N/2+2) & \ldots & p_0(N) \end{bmatrix} \tag{4}$$

$\boldsymbol{A}'$ is the filtered signal.

Since the SVD is a fully invertible mathematical operation, the remaining components are restored after PSVD filtering, and the signal no longer contains the components that do not relate to arc faults but hinder the characteristic analysis of the remaining components with masking effects caused by their overwhelming energy proportions [35]. The empirical mode decomposition (EMD) analysis did not extract enough information from the arc-fault data when the aforementioned masking components were not filtered. Excluding the phase shift, the arc-fault signal is very similar to the normal signal in terms of contrast; hence, they are not quite distinguishable. However, once the masking components are filtered, the features of the arc-fault signal extracted by the EMD demonstrate a more sophisticated pattern, and the information can be accessed is much more plentiful. At this point, the empirical features of the arc-fault signal contrast well with the normal signal, and classifying them is easy.

A demonstration of the filtering effects of the PSVD shown by the composites of correspondent EMD sequences of unfiltered and filtered signals is depicted in Fig. 2. The load of the samples in Fig. 2 is electronic dimming light, and the rated current amplitude is 5 A.

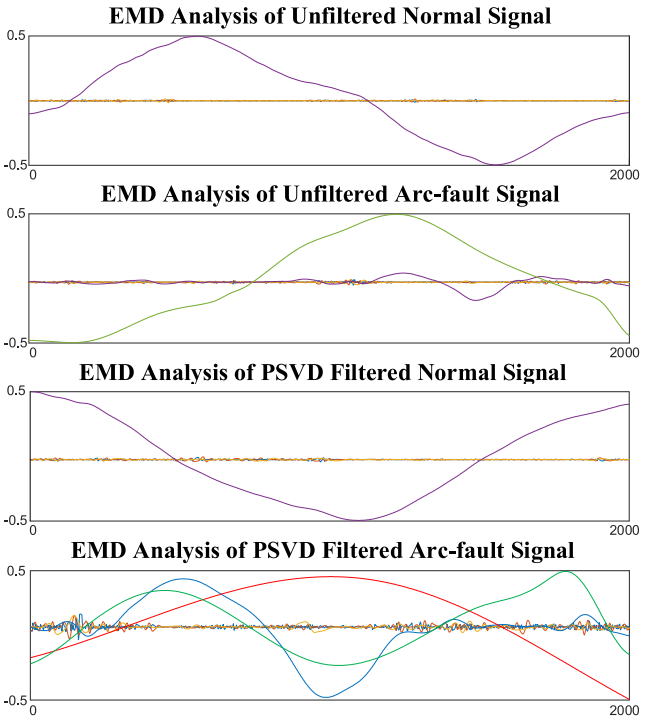

FIGURE 2. Demonstration of PSVD filtering effects by performing EMD on unfiltered and filtered normal and arc-fault signals.

The values in Fig. 2 are standardized to between -0.5 and 0.5 with the mean value of 0, the horizontal axis corresponds to the index values of 2,000 data within one sampling window. The demonstration proves that the PSVD is capable of considerably reducing the masking effects by filtering the components not closely related to arc-fault features, though they possess the dominant energy proportions in the original signal.

C. EMPIRICAL MODE DECOMPOSITION

The right decision of the tools for the extraction of the arc-fault features is the most critical part in developing a successful detection method. Lala and Karmakar [36] proposed an arc-fault detection method that extracts features by empirical mode decomposition (EMD) and makes diagnoses by neural networks (NNs); determining the results, the method was a success; however, the research subject was high-impedance arc faults, which are a fault type more distinguishable than weak arc faults. Another method that extracts features by the EMD and classifies signals by the support vector machine (SVM) was also introduced in [37].

EMD is a mathematical tool invented by Huang et al. [38] in 1998; it approximates IMF sequences layer-by-layer by the differential sequences between the spline lines of local maxima and local minima minus the mean of the current layer. It has been shown by Equations (3.2) and (3.3) in [38] that an IMF sequence after the Hilbert transform can be expressed as an analytic signal $\boldsymbol{Z}(t)$:

$$\begin{aligned} Z(t) &= \mathrm{X}(t) + i\mathrm{Y}(t) = \alpha(t)\mathrm{e}^{i\theta(t)}, \\ \alpha(t) &= [\mathrm{X}^2 + Y^2(t)]^{1/2}, \end{aligned} \tag{5}$$

$$\theta(t) = \arctan(\frac{Y(t)}{X(t)}) \tag{6}$$

Then, to perform a Fourier transform on such an analytic signal $\boldsymbol{Z(t)}$, the result $\boldsymbol{W(\omega)}$ sequence has the instantaneous frequency of the original signal as the maximum contribution according to the stationary phase method, $\boldsymbol{\omega}$ being the instantaneous frequency sequence, and $\boldsymbol{\theta}$ being the frequency sequence, as shown by Equation (7), which corresponds to Equation (4.1) in [38].

$$W(\omega) = \int_{-\infty}^{\infty} \alpha(t) e^{i\theta(t)} e^{-i\omega t} dt \tag{7}$$

In summary, the IMF sequence of each layer reflects partial instantaneous frequency information of the original signal in the time-frequency domain. EMD is a widely recognized feature extraction tool in recent years because it reliably analyzes the signals by layers of the intrinsic mode function (IMF) sequences, and it can be executed quickly. Since the two merits of the EMD perfectly satisfy the requirements of the method design in this study, the EMD is selected as one of the feature extraction tools for the proposed method.

The comparison research of the IMF sequences (EMD components) of the collected data in this study is demonstrated in Fig. 3, with the load of the experimental samples being the electronic dimming light (EDL), and the rated current amplitude being 5A. The IMF sequences are distorted compared to the ones extracted from a normal signal, and the pattern of each IMF sequence no longer shows ups and downs in correspondence with the AC current; instead, it emphasizes a peak that clearly resembles the arc. However, the clear contrast depicted in Fig. 3 does not always exist in other sampling windows, especially when the VI characteristics of arc-fault samples are almost identical to the normal ones at the beginning of a weak arc fault; therefore, relying on EMD components alone is not sufficient for accurate detection with the sampling window limited to one current cycle for fast execution.

Su and Xu [39] also presented an EMD-based arc-fault detection method, which extracts specific IMF sequences by the EMD and then calculates the mathematical indices from the coefficients of the sequences as arc-fault features. The results were acceptable; however, the method was too customized, and the optimal number of IMF layers for each experimental setting was decided by experimental results, which made the method prone to overfitting and not adaptable. To overcome the same dilemma, the method proposed in this study does not manually select the signals to separate them into categories in accordance with the experimental settings. The data collected from all experiments are used to train, verify and test the networks without manual adjustments, regardless of the differences in experimental conditions.

D. EMPIRICAL WAVELET TRANSFORM

Mandic et al. continued the research on empirical mode decomposition and presented a study result of performing

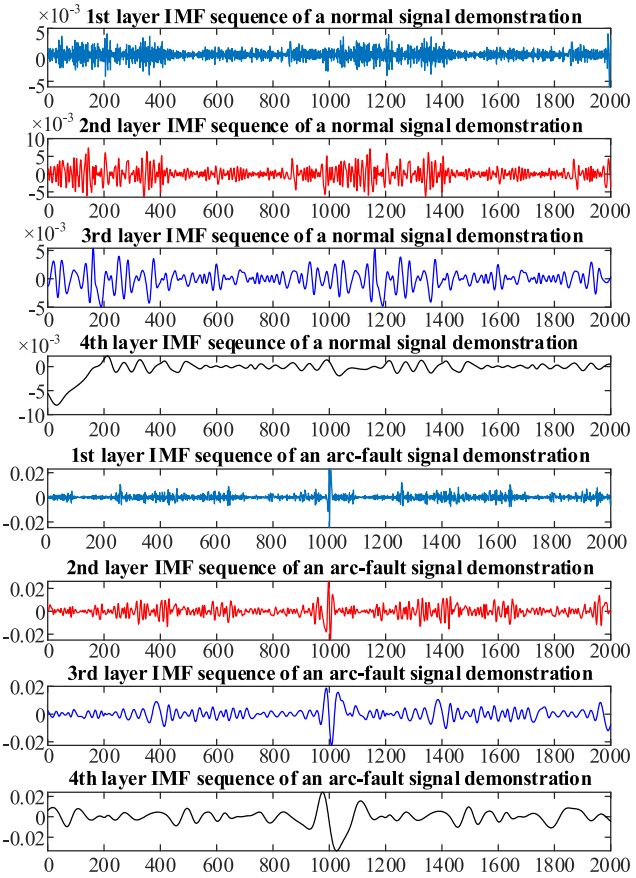

FIGURE 3. Demonstration of IMF sequences of PSVD filtered normal and arc-fault signals extracted by EMD.

EMD to analyze multivariate signals in the time-frequency domain. It is worth mentioning that Huang, as the founder of EMD, was also a member of this research team [40], in which it was shown that the performance of the traditional EMD method could be improved by combining the EMD with the discrete wavelet transform (DWT). However, the DWT is not as fast as the EMD, and using both the EMD and DWT for feature extraction will slow down the detection. A comprehensive survey of empirical analysis methods [41] suggests that the empirical wavelet transform (EWT) can be a good substitution of the DWT because it extracts the layer-by-layer wavelet coefficients as compliments to the EMD components for feature extraction as well, but it can be implemented to run as fast as the EMD.

Gilles invented the EWT in 2013 [42]; the empirical wavelets are bandpass filters each constructed according to the empirical scaling function, and the empirical scaling function and wavelets are defined by Equations (4), (5), and (6) in [42]. The empirical scaling function of the EWT is expressed as follows:

$$\widehat{\phi}_n(\omega) = \begin{cases} 1 & \text{if } |\omega| \le \omega_n - \tau_n \\ \cos\left[\frac{\pi}{2}\beta\left(\frac{1}{2\tau_n}(|\omega| - \omega_n + \tau_n)\right)\right] & \\ 0 & \text{otherwise} \end{cases} \tag{8}$$

The empirical wavelets can be described by the following equations:

$$\widehat{\psi} = \begin{cases} 1 & \text{if } \omega_n + \tau_n \le |\omega| \le \omega_{n+1} - \tau_{n+1} \\ \cos\left[\frac{\pi}{2}\beta\left(\frac{1}{2\tau_{n+1}}\left(|\omega| - \omega_{n+1} + \tau_{n+1}\right)\right)\right] & \\ & \text{if } \omega_{n+1} - \tau_{n+1} \le |\omega| \le \omega_{n+1} + \tau_{n+1} \\ \sin\left[\frac{\pi}{2}\beta\left(\frac{1}{2\tau_n}\left(|\omega| - \omega_n + \tau_n\right)\right)\right] & \\ & \text{if } \omega_n - \tau_n \le |\omega| \le \omega_n + \tau_n \\ 0 & \text{otherwise} \end{cases} \tag{9}$$

$$\beta(x) = \begin{cases} 0 & \text{if x } \le 0 \\ & \text{and } \beta(\mathrm{x}) + \beta(1-\mathrm{x}) = 1, \forall \mathrm{x} \in [0,1] \\ 1 & \text{if x } \ge 1 \end{cases} \tag{10}$$

The EWT extracts different modes of a signal by an adaptive wavelet filter bank, which is a new wavelet analysis tool that extracts information in the time-frequency domain by wavelet coefficients in a layer-by-layer manner instead of the traditional decomposition by frequency bands. A EWT-based method that resolves the spectrum subdivision problem by morphological filtering enhancement was proposed in [43]. In this research, it was stated that EWT provides a consistent decomposition by wavelet analysis, while EMD sometimes exhibits diverse results and it can be difficult to interpret the information, so EMD and EWT can be applied together for improved feature extraction. The method of arc-fault detection using a twin support vector machine was introduced in [44]; this method also utilized the EWT as the base approach for feature extraction. As a result of the successful examples and with the aim of fast and comprehensive feature extraction in the time-frequency domain and the caution of not overly processing the features so that the trained machine learning classification tool is more resilient to the challenge of overfitting, the EWT was also chosen as a feature extraction tool in this research.

The demonstration of normal and arc-fault EWT sequences is displayed in Fig. 4. The data samples used for Figs. 3 and 4 are the same to show the differences and resemblances between the EMD and EWT components in comparison. Judging by the results, the EWT coefficients complement the information obtained by the EMD well such that the detection accuracy is enhanced by combining the EWT with the EMD, and the detection speed does not show an apparent slow-down due to the fast execution of both approaches.

E. FEATURE EXTRACTION AND CLASSIFICATION BY NEURAL NETWORKS (NN)

To further improve the detection accuracy without a costly trade-off on the executional speed, the fast Fourier transform (FFT) has been incorporated as another feature extraction tool because it is at least equally as fast as the EMD and helpful to extract features in the frequency domain [34]. Referring to the proposals in [34] and [39], verified by the experimental results, each sequence extracted by the EMD and EWT is computed into sum and kurtosis, while each FFT sequence

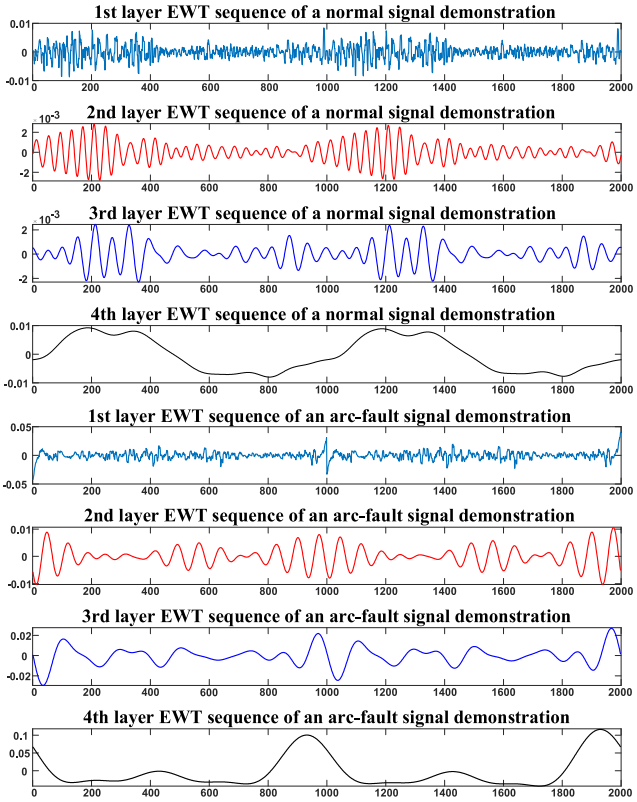

FIGURE 4. Demonstration of EWT sequences of PSVD filtered normal and arc-fault signals.

is computed into sum and standard deviation, since kurtosis is not meaningful in the frequency domain.

An overview of the complete feature extraction and machine learning (ML) classification based on the extracted features in this study is shown in Fig. 5. Due to the increased amount of extracted features, the most suitable classification tool is no longer the support vector machine (SVM), as presented in [34] and [35]. Neural networks (NNs) are selected as the classification tool for the proposed method to make diagnoses for each sample after integrating the features. The influences of different sizes of the sampling window are shown in Fig. 6, and the comparison of the two ML classification tools with the same features and sampling winnow size is depicted in Fig. 7.

As shown in Fig. 6, the detection accuracy is considerably improved from 81.47% to 100% by increasing the size of the sampling window from 1,000 data points to 8,000 data points with a sampling frequency of 100 kHz in the 50 Hz AC system. When the sampling window size is increased from 2,000 or one current cycle to 8,000 or four current cycles, the detection accuracy is improved from 96.12% to 100% in this comparative test, but the detection time is increased by nine times, which is a costly trade-off. With the sampling window size increased from one current cycle to four, and the average detection time increased to 0.306 s, which corresponds to at least 30 current half-cycles in a 50 Hz AC system, also

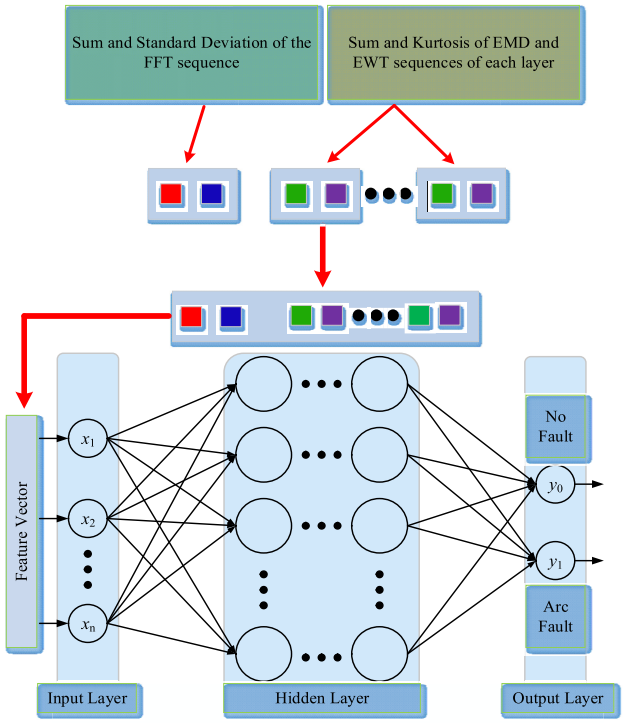

FIGURE 5. Overview of empirical feature extraction and NN classification of the proposed method.

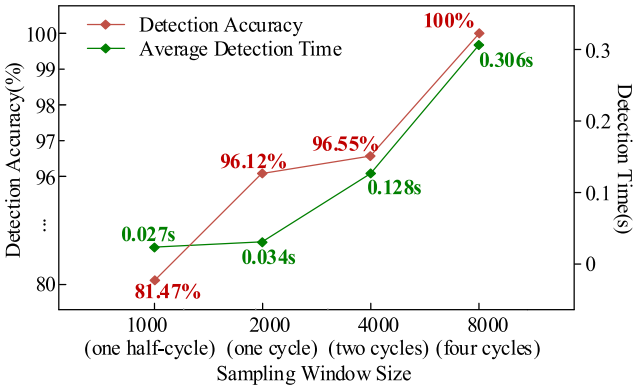

FIGURE 6. Research comparison of detection accuracies and times of the proposed method on different sampling window sizes.

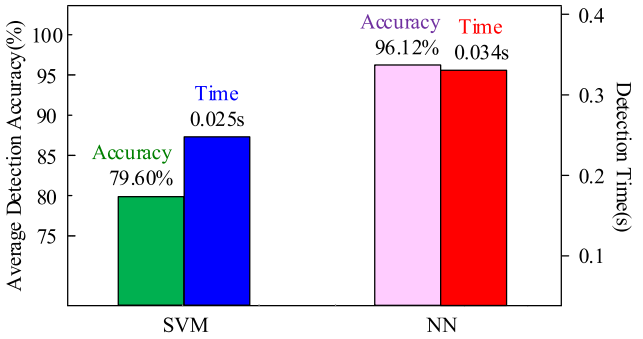

FIGURE 7. Performance comparison of SVM and NN to process extracted features as ML classification options.

considering the sampling time, an arc is possibly allowed to burn for more than 40 half-cycles before being detected, then the direct application of the algorithm in China is disqualified by the current Chinese standard for AFDDs, which requires an arc fault of a current amplitude below 75 A to be detected within 12 half-cycles [33]. Based on the results, the sampling window size is set to be one current cycle.

The NN is now a better ML classification tool than the SVM, as illustrated clearly in Fig. 7; the SVM still has the speed advantage, but the poor accuracy eliminates it as a candidate ML tool for the proposed method. The NN applied for the proposed method is the backpropagation neural networks (BPNN) with the settings of one hidden layer, a maximum epoch number of 10,000, a learning rate of 0.01, and an error margin of 0.00000001; the parameters are decided by trial-and-error automatic test runs. The node number in the input layer is decided by the layer numbers of the signals decomposed by the empirical analysis (EA), which is 19 (18 features plus 1 label) in this study, and the node number of the hidden layer is set as twice the node number in the input layer plus one, which is 39, according to Kolmogorov's theorem explained in [45]. Although there are more advanced parameter optimization approaches introduced in previous studies, including the differential evolutionary cooperative coevolution (DECC) composed of the quantum evolutionary algorithm (QEA) and genetic algorithm (GA) [46], and the combination of the variable neighborhood search and the nondominated sorting genetic algorithm [47], the scale of the parameter matrix in this study is not large enough for the merits of the abovementioned approaches to become apparent, and the parameter tuning for the ML tool is not as influential as the feature extraction in detecting arc faults verified in [34] and [35].

F. IMPLEMENTATION PROCESS AND FLOWCHART

The purpose of this study is to continuously develop a fast and reliable arc-fault detection method on the foundation of previous studies, [34] and [35]. The PSVD-FFT method proposed in [34] addressed the weakness of slow execution of the WASVD-CAN method proposed in [35] and substantially improved the detection speed. However, the PSVD-FFT method still needs to be modified in regard with the following drawbacks: the maximum number of responsive current cycles to detect an arc fault is 12 due to the dynamic design, meaning that in the worst case scenario, an arc fault cannot be detected until it has been burning for 24 current half-cycles, plus the executional time of the algorithm; the accuracy still has room for improvement, and the detection time can be further reduced. The PSVDEA-NN method proposed in this study has solved each of the aforementioned drawbacks of the PSVD-FFT method with excellent detection accuracy, even faster detection speed, moreover, the responsive current cycle for an arc fault is fixed to be 1. Therefore, the newly designed method has overcome the weaknesses of the previous studies in [34] and [35], and the purpose of this study is fulfilled. A more comprehensive comparison between the

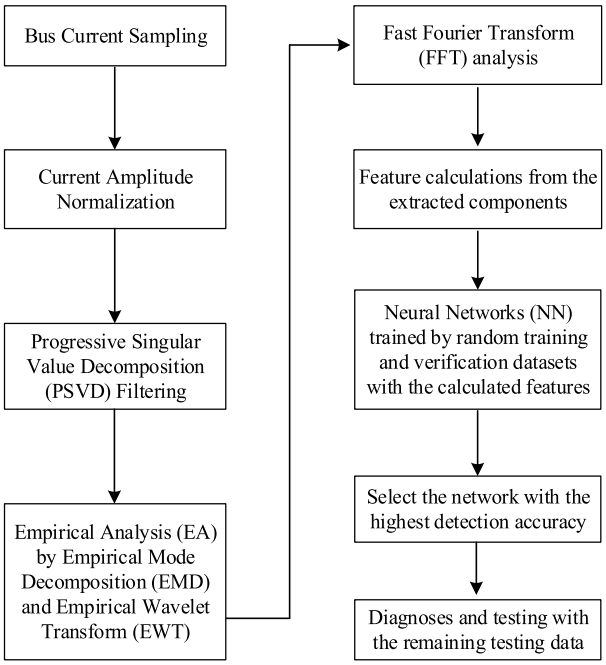

FIGURE 8. Logic design and step explanations of the proposed PSVDEA-NN method.

WASVD-CAN, PSVD-FFT, and PSVDEA-NN methods with other selected methods is presented with details in the next section. The logic design of the proposed method is shown in Fig. 8. Fig. 9 is the complete flowchart of the proposed method.

This study adopts a design principle similar to that of previous studies, which uses relatively simple mathematical tools to reduce the complexity of the problem and then constructs feature vectors to be processed by ML classification. For example, Chen et al. developed a method for hyperspectral images of which principal component analysis (PCA) is employed to reduce the complexity of hyperspectral images, and the local binary pattern (LBP) is used for constructing feature vectors to be processed by the kernel extreme learning machine (KELM) [48]. The proposed method utilizes the PSVD, which is the fastest form of the SVD, along with fast empirical analyses, including the EMD and EWT, as well as the FFT, one of the fastest analytical tools in the frequency domain. In addition, the trained neural network takes little time to make each diagnosis by computing one arithmetic equation with parameters tuned during the training. This design enables the proposed method to detect arc faults in a timely and accurate manner.

III. EXPERIMENTS AND ANALYSES

A. EXPERIMENTAL CONDITIONS

There is a total of 2,320 datasets (sampling windows) generated from the experiments in this study to evaluate the proposed method and parallel comparison. The experiments are composed of various load settings, current amplitudes, circuit layouts, and several types of arc faults simulated by different arc generators. The voltage-current waveform demonstration of realistic sampling during experiments with different conditions is depicted in Fig. 10, and the conditions of each set of experiments are summarized in Table. 2. The experiments are also incorporated in two previous studies, [34], [35]. Fig. 10 corresponds to Fig. 10 in [34] and Fig. 15 in [35]. However, in [34] and [35], the experiments of each set of conditions are used to test the performances of the methods individually, but in this study, all of the experimental data are used to evaluate the proposed method and the methods for comparison altogether. Considering the nature of the machine learning (ML) algorithms and the AC system characteristics at the user end, the frequent shift of loads and fluctuations of the bus current amplitudes should be common, and ML algorithms are particularly good at classifying data with repetitive patterns; therefore, the methods should be evaluated by their performances on arc-fault detection within samples from all of the experiments for more realistic simulation. The sampling window size is determined to be 2,000 data points, which is one current cycle with the sampling frequency set to 100 kHz according to the research comparison shown in Fig. 6.

It is worth mentioning that among the eleven experimental sets there is only one parallel arc-fault type. The parallel arc faults generally have higher arc current magnitudes and generate more energy under the same circuit conditions, in most cases it is easier to detect parallel arc faults than series ones. However, the arc current amplitudes are not measured, only the bus current is measured, and the current amplitudes in Table 2 are the rated current amplitudes of the loads. Since the location of potential arc faults cannot be decided beforehand, arc faults are detected by the features extracted from the bus current. Arc faults are random and the energy keeps being emitted in different forms and directions from arcs, so the impact caused by parallel arc faults on the bus current is not as large or regular as short-circuit faults. To add a parallel arc-fault experiment is to examine whether the algorithm can successfully recognize parallel arc faults when the majority of faults are series ones.

The strong arc-fault signals with bus-current fluctuations that are obviously larger than the ones of normal load operations are excluded, because the emphasis of this research is to detect weak arc faults from mixed signals of different load operations by alternations in the patterns of the bus current, without depending on current magnitudes. The arc faults that cause abnormally large bus-current fluctuations can be detected by a circuit-breaker or residual current circuit-breaker with overcurrent protection. However, arc faults, especially the ones in early stages, are not necessarily accompanied by apparent changes in the magnitudes of bus-current fluctuations, thus overcurrent protection cannot be triggered.

B. DESCRIPTION OF THE METHODS SELECTED FOR PERFORMANCE COMPARISONS

Three previously established arc-fault detection methods and one earlier version of the proposed method are selected

TABLE 2. Summary of experimental conditions and data composition.

Load Type	Arc-fault Type	Rated Current Amplitude	Data Composition
Electronic Dimming Light	series	5A	120 normal samples, 120 arc-fault samples
Resistors	parallel	15A	120 normal samples, 120 arc-fault samples
Motor	series	14A	120 normal samples, 120 arc-fault samples
Fluorescent Light	series	8A	120 normal samples, 120 arc-fault samples
Hand Drill	series	6A	100 normal samples, 100 arc-fault samples
Halogen Lamp	series	9A	100 normal samples, 100 arc-fault samples
Resistors	series	5A	100 normal samples, 100 arc-fault samples
Switching Power Supply	series	14A	100 normal samples, 100 arc-fault samples
Vacuum Cleaner	series	20A	60 normal samples, 60 arc-fault samples
Electronic Dimming Light, Fluorescent Light, and Halogen Lamp in parallel	series	5A electronic dimming light, 9A halogen lamp, and 8A fluorescent light	100 normal samples, 100 arc-fault samples
Switching Power Supply and Vacuum Cleaner in parallel	series	14A switching power supply and 20A vacuum cleaner	120 normal samples, 120 arc-fault samples

for parallel comparison, including the EMD-PNN [39], the WASVD-CAN [35], the PSVD-FFT [34], and the PSVDEA-SVM; except for the PSVDEA-SVM, the other methods are introduced by published articles. For the sake of a fair comparison, all algorithms are reprogrammed to be executed on the same computational platform, and examined by exactly the same experimental data.

The EMD-PNN method calculates the standardized parameters from each of the specific layers of the extracted intrinsic mode function (IMF) sequences to maximize the margin between normal signals and arc-fault signals, and the diagnoses are made by probabilistic neural networks (PNN) with the parameters as features. The original version of the EMD-PNN extracts features from specific IMF layers by empirical mode decomposition (EMD) for each load setting according to the characteristic analysis beforehand. However, in this study, the data contain a variety of load settings, in contrast to [39], where each load setting is studied and tested separately. The original approach is no longer suitable; relying on manual adjustment for each load setting deprives the method of the functionality in realistic applications. Now the test data are the normal and arc-fault signals from eleven experiments of conditions distinct from one another, and it is impossible to manually decide which IMF sequences to be included, therefore, the optimal IMF layer number is decided by an exhaustive search on the outcomes of the probabilistic neural networks (PNN) trained with IMF sequences of different layer numbers. This process is very time-consuming, but it is the necessary improvement for the method to be usable in detecting arc faults within mixed samples from experiments with distinctively different settings.

The WASVD-CAN method normalizes current amplitudes and decomposes the signals by wavelet analysis (WA), then applies singular value decomposition (SVD) to the wavelet coefficient sequences and locates the corresponding coefficients of the irrelevant components with large energy indices that cause masking effects, including the AC/DC components, by entropy calculation. Then, the method filters those components by setting the coefficients to zero before further reducing the environmental and systematic influences by subtracting one calculated standard signal base from each wavelet coefficient sequence. Since WA and SVD are both fully reversible mathematical operations, the signals with components irrelevant to arc-fault detection filtered are reconstructed from the remaining coefficients for feature calculation. The features are passed to the support vector machine (SVM) for diagnoses. Per the results presented in [35], the method can achieve high accuracy by carefully eliminating all of the components that are not closely related to arc-fault detection to maximize the difference between normal signals and arc-fault signals. However, this method is slow, because the conventional SVD, WA and reconstruction processes on each signal consume too much time. It has been shown in [34] that with more advanced hardware, the execution of the method can be accelerated, but the detection speed of this method is still a downside compared to some other methods with the same data on the same platform. Moreover, the original sampling window size for the WASVD-CAN in [34] is 8,000 data points with a sampling frequency of 100 kHz, which corresponds to four current cycles; when the sampling window size is decreased to 2,000 data points, the detection accuracy of the method shows a cliff descent. The dependence on a larger sampling window is a weakness of the method. The more current cycles to make a single detection are demanded, the more sampling time is needed regardless of the sampling frequency; when the method requires information from more current cycles to detect an arc fault, the potential burning time of the arcs is prolonged.

To solve the imbalance between the detection accuracy and speed of the WASVD-CAN method, the PSVD-FFT method starts with the current amplitude normalization, and then the signals are analyzed by the fastest form of the SVD, progressive singular value decomposition (PSVD), in a recursive manner. In each round of recursion, the signal under decomposition is filtered by half, and a singular value is extracted

TABLE 3. Overall detection accuracies and average detection times of selected methods in comparison.

Method	Detection Accuracy (%)	Average Time (s)
EMD-PNN [39]	68.36	0.199
WASVD-CAN [35]	49.96	0.151
PSVD-FFT [34]	77.12	0.016 - 0.047
PSVDEA-SVM	79.60	0.025
PSVDEA-NN	96.12	0.034

as a feature, with the optimal amount of recursions decided empirically by comparative studies. The feature extraction is enhanced by the fast Fourier transform (FFT), and all of the features are passed to the SVM to diagnose potential arc faults within each small diagnostic window. Then, the results of the small diagnostic windows are integrated into the structure of the double diagnostic window frame (DDWF) to reduce the most common errors in the detection of weak arc faults, which are the false-negative type errors. As illustrated by the results in [34], the PSVD-FFT achieved a detection speed that is considerably faster than the WASVD-CAN with a satisfactory detection accuracy. The weakness of the PSVD-FFT method is that, to maintain high detection accuracy, the DDWF is necessary; however, this structure increases the number of maximum current cycles allowed to detect an arc fault, potentially prolonging the burning time of an arc, which can lead to a safety hazard. Nevertheless, of course, with the high detection accuracy and fast detection speed, this method still has its practical value. The sampling window size of the PSVD-FFT method in [34] is 4,000 data points with a sampling frequency of 100 kHz, which corresponds to two current cycles; the detection accuracy decreases when the sampling window size is reduced to 2,000 data points.

The contrast between the proposed PSVDEA-NN and PSVDEA-SVM is already depicted in Fig. 7. The only difference between the two is the choice of the machine learning (ML) tool for making the final diagnoses, and it is also included here for the sake of analysis.

The comparative test results are displayed in Table 3. The algorithms of the methods are written in MATLAB 2021 and executed on a laptop computer with one Intel i7-7700HQ CPU and 24 GB RAM. Each window sampling takes 0.02 s with the sampling frequency of 100 kHz.

The proposed PSVDEA-NN method achieved excellent performance in both detection accuracy and speed with the sampling window size of 2,000 data points and sampling frequency set to 100 kHz, which corresponds to only one current cycle. In AC systems, one current cycle is almost the minimal sampling window size for any heuristic detection method without special sampling processes, since the features extracted from normal signals are to be compared with those extracted from arc-fault signals for the algorithms to adaptively learn the differences; hence, serious information loss is bound to happen when the sampling window size is less than one current cycle because the half-cycles have quite different patterns even when no faults have occurred.

C. ANALYSIS OF THE RESULTS

Table 3 shows the detection times and accuracies of the PSVDEA-NN method proposed by this study and the methods for comparison. Per the results, the overwhelming dominance of the proposed method in arc-fault detection with the sampling data window limited to one current cycle is clearly illustrated, partially because other methods were designed to function with larger sampling window sizes. In the area of DC arc-fault detection, if the sampling subject is the DC bus current, the information of the system contained in the current cycles does not concern the sampling window size because there are no current cycles, so the sampling window size can be as small as 1,000 data points with a sampling frequency of 100 kHz [23] or even smaller. However, in the area of AC arc-fault detection, if the method resolves the problem in a heuristic manner rather than in a deterministic or empirical manner to diagnose arc faults by capturing changes in the pattern caused by the arcs, a sampling window size smaller than one current cycle requires modified sampling approaches. As explained in earlier sections, a smaller sampling window size indicates less sampling time, and more importantly, more sensitivity to burning arcs because the minimum number of current cycles a method allows arcs to burn cannot be less than the number of AC current cycles required for sampling.

It has also been shown by Fig. 13 in [35] that the accuracy of the WASVD-CAN method is approximately 50% when the sampling window size is 2,000 data points; the method fails to classify, thus all of the signals are labeled the same, but the accuracy of the WASVD-CAN method increases rapidly from 49.96% to over 95% when the sampling window size increases from 2,000 data points to 8,000 data points. The accuracy of the EMD-PNN is 68.36% because it is degraded not only by insufficient data in each sampling window but also by mixed load settings and current amplitudes. The original design of the method adapts to each experimental condition by abundant manual analyses and then the separately trained PNN networks take the test by signals from each set of the experimental conditions. A method such as this can still be used in realistic situations if once the application scenario is adapted, it does not change often. In contrast to the PSVD-FFT that extracts the singular values of the PSVD as the arc-fault features, the PSVD part of the proposed method is utilized as the filter, the original design of the PSVDEA-SVM method is to work with the sampling window size of 4,000, and the downsized sampling window does affect the detection accuracy. The detection accuracies of PSVD-FFT and PSVDEA-SVM are 77.12% and 79.60%, respectively, which are hardly passable. Since the only difference between the PSVDEA-NN and PSVDEA-SVM is the ML tool, it is a good demonstration of how the neural networks (NN) outperform the support vector machine (SVM) in integrating relatively numerous features. The proposed PSVDEA-NN method is the only method that has achieved a satisfactory detection accuracy with the restricted condition of detecting arc faults within each current cycle, and the outstanding

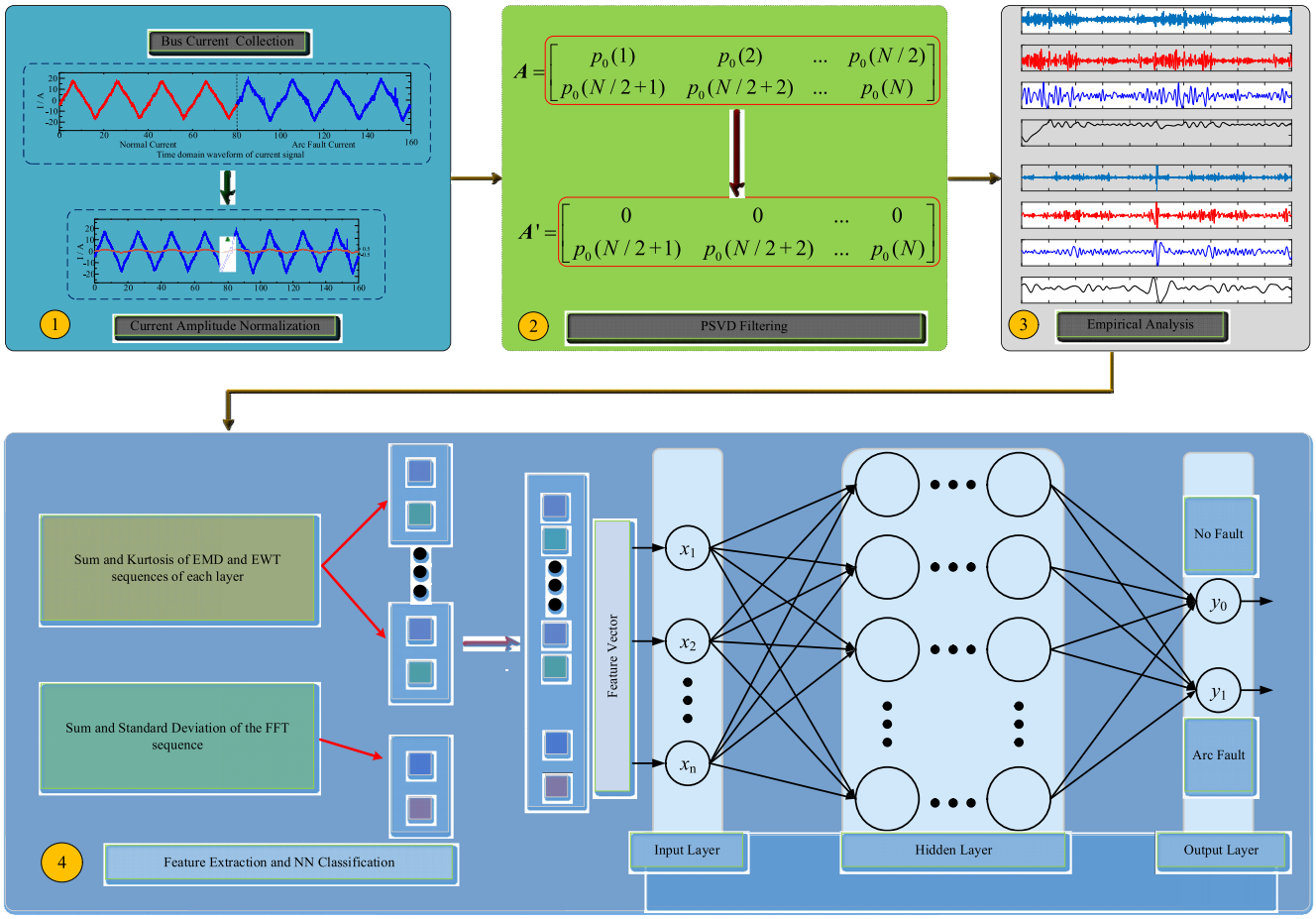

FIGURE 9. Complete flowchart of the proposed PSVDEA-NN method.

96.12% detection accuracy is ahead of all the other methods in comparison by a wide margin.

The detection times of the methods in comparison vary, the EMD-PNN has the slowest average detection time of 0.199 s, and the WASVD-CAN is faster, though not by much, with the average detection time of 0.151 s, and they are the slowest among the methods in comparison. The EMD-PNN is slow because the optimal IMF layer number decided dynamically can be large, and customization of the EMD is necessary, then the repetitive feature extraction by the customized EMD takes a heavy toll on the detection speed. The WASVD-CAN is slow since it performs the Hankel matrix form of the singular value decomposition (SVD) on each signal as the most time-consuming part of the feature extraction, and this became the inspiration of the PSVD as a fast substitution. The PSVD-FFT can be faster than the proposed method with an average detection time between 0.016 s and 0.047 s. Even if the average detection speed is slower than the PSVDEA-NN for the diagnoses made by three consecutive sampling windows in the DDWF structure [34], the average detection speed of the diagnoses made by only one sampling window is about 50% faster than the proposed method. However, with more powerful computational tools, the execution of the algorithms can be accelerated, but the DDWF structure potentially allows up to three sampling windows to confirm a diagnosis, which correspond to three consecutive current cycles, and the sampling time of the current cycles is restricted by the AC current frequency thus cannot be accelerated. The PSVDEA-SVM, although faster than the PSVDEA-NN, with an average detection time of 0.025 s over 0.034 s, is nevertheless not in the same rank as the proposed method due to its poor detection accuracy. It is worth mentioning that some of the methods in comparison perform well in regard with detection speed because the sampling window is much smaller than their original designs, and a smaller sampling window size not only reduces the sampling time but also considerably decreases the amount of data processed in each iteration, which is in polynomial or exponential proportion to the executional time. If the sampling window size increases, the average detection speeds of the methods in comparison will be much slower, and the detection accuracies of these methods are far inferior to the proposed method with the small sampling window size. For example, the average detection time is reduced from 0.068 - 0.198 s of the PSVD-FFT method with a sampling window size of 4,000 data points to 0.016 - 0.047 s with a sampling window size of 2,000 data points, and the 96.18%

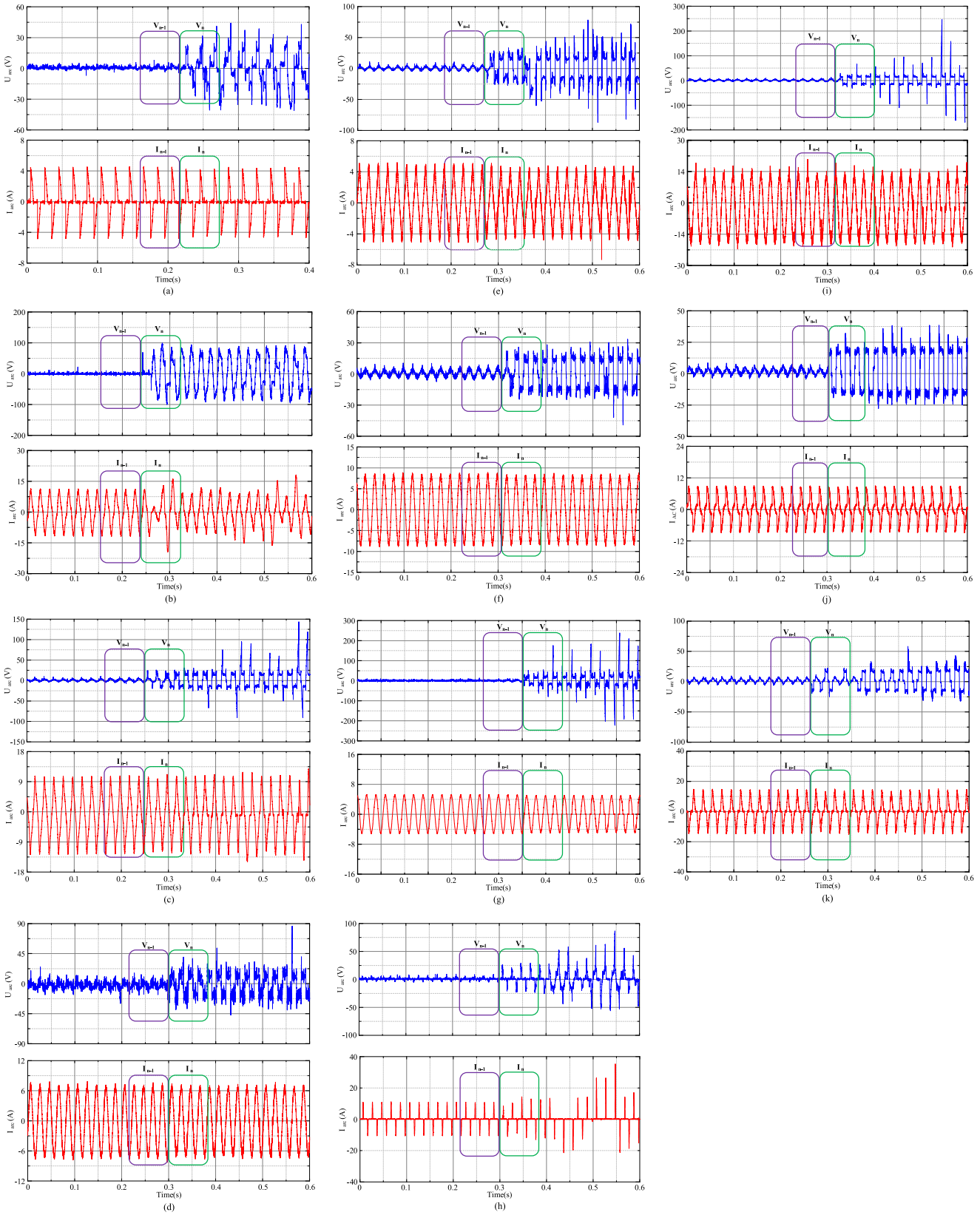

FIGURE 10. Voltage-current waveform demonstration of adjacent sampling windows before and after arc generation in each experiment. (a) Electronic Dimming Light. (b) Resistors for Carbonized-path Arc Generator. (c) Squirrel-cage Induction Motor. (d) Fluorescent Light. (e) Hand Drill. (f) Halogen Lamp. (g) Resistor for Rods-pulling Arc Generator. (h) Switching Power Supply. (i) Vacuum Cleaner. (j) Electronic Dimming Light, Fluorescent Light, and Halogen Lamp in Parallel. (k) Switching Power Supply, and Vacuum Cleaner in Parallel.

detection accuracy of the PSVD-FFT method with the 4,000 data or two current cycles sampling window size is close to the 96.55% accuracy of the PSVDEA-NN with the same sampling window size, according to the results presented in [34]. However, when the sampling window size is reduced to one current cycle, the proposed method does not suffer from a noticeable decrease in the detection accuracy (from 96.55% to 96.12%), where the detection accuracy of the PSVD-FFT drops from 96.18% to 77.12%.

The proposed method is the only candidate among the five methods in parallel comparison to perform well in regard to both of the detection accuracy and speed, with an average time of 0.034 s to make a single diagnosis. It has consistently detected arc faults accurately from the mixed data generated by eleven experiments, each with a unique set of experimental conditions that represents a category of realistic arc-fault scenarios. The detection accuracy of the proposed method is 16.52% higher than the method that switches the ML tool from the NN to SVM; moreover, it is at least 19% higher than the established methods proposed by previously published articles and improves the detection accuracy comparatively by at least 24.63%. This study successfully invents a heuristic method for the detection of weak arc faults in AC systems, which limits the sampling window size required for accurate detection down to only one current cycle. The breakthrough in the sampling window size substantially shrinks the sampling time, and the current cycles of the method allow an arc to burn before being detected. With the sampling window size being just one AC current cycle, the PSVDEA-NN method achieved a 96.12% accuracy in detecting weak arc faults on a total of 2,320 samples of different load settings, arc-fault types, circuit layouts and current amplitudes. Since the executional time is drastically influenced by the data contained in each sampling window, this also enables the method to detect arc faults much faster. The average detection time of 0.034 s is close to the sampling time of 0.02 s with the current sampling window size of one current cycle and sampling frequency of 100 kHz. If the executional speed is faster than sampling, the method can be used to monitor the conditions of the system in real-time and detect arc faults with no delays.

The most relatable application scenario of the proposed method is to function as the incorporated algorithm of AFDDs or circuit breakers in low voltage AC systems. However, since this method does not depend on zero-crossing distortions or current magnitudes, it has the potential to be applied in DC systems as well, referring to a previous research that combines the central neural networks (CNN) and long-short term memory (LSTM) to construct a deep learning (DL) approach for the detection of series arc faults in DC systems [49]; or another example presented in [50], which extracts features from the bus current and VI characteristics of the load in a DC experimental circuit, to detect parallel arc faults by artificial intelligent algorithms. The proposed method is adaptable to different application scenarios because it is accurate, fast, and does not rely on arc-fault features exclusive to AC systems.

IV. CONCLUSION

This research inherits the knowledge from [34] and [35], aiming for a detection method for AC weak arc faults with excellent accuracy and speed. The method presented in this study has progressed forward to reduce the average detection time even more on top of the fast execution in [34], with the realization that the key point in further accelerating the diagnosing process is to downsize the sampling window. This research successfully modified the traditional filtering and feature extraction technique by the original PSVD filter and the combination of empirical analyses and BPNN classification, so that features extracted from just one current cycle of the AC bus current are sufficient for fast and reliable arc-fault diagnoses.

One of the contributions of this study is the design of using the fastest form of the singular value decomposition (SVD), the progressive SVD (PSVD), to filter the current components that cause masking effects on the feature extraction, which has been proven to be effective and fast. Another contribution is to utilize fast compound empirical analysis (EA) with the help of a fast Fourier transform (FFT) to extract arc-fault features. The third contribution is the implementation of the neural networks (NN) to repetitively select random training, verifying and testing datasets from the pool of samples. Then, the neural network selected is the one with the highest detection accuracy from numerous repetitions, and the results show strong support of the idea.

Although the proposed method has withstood the challenge of detecting weak arc faults from over two thousand samples of various experiments with different experimental conditions and dominated the comparison test with excellent accuracy and speed, the following three subjects still need to be researched to further improve the proposed method so that it can become practical for realistic applications: (1) The average executional time of the method is still longer than the sampling time, which is a frontier for real-time arc-fault detection without delays. The executional time can be shortened to below the sampling time by the advancement of hardware alone or a combination of algorithm modifications and hardware upgrades; to prepare the proposed method for real-time detection or system monitoring tasks, the average detection time or even better, the maximum detection time, has to be less than the sampling time. (2) The adaptiveness in classifying data generated by scenarios absent from the experimental data is unverified. The proposed method effectively learns to diagnose weak arc faults from the signals of different experiments, each experiment represents a category of realistic scenarios with abundant data, but its ability to generalize a pattern for signals from novel scenarios with inadequate data is yet to be tested. (3) In realistic environments, there can be interference factors that are not simulated by the experimental platform, and the composition of signals can be a lot more complex, the method must be equipped with necessary anti-interference solutions to remain functional.

REFERENCES

[1] T. Zhang, R. Zhang, H. Wang, R. Tu, and K. Yang, "Series AC arc fault diagnosis based on data enhancement and adaptive asymmetric convolutional neural network," *IEEE Sensors J.*, vol. 21, no. 18, pp. 20665–20673, Sep. 2021.

[2] J. Swart, J. Loud, and D. Slee, "Arcing and fires—Case studies," in *Proc. IEEE Symp. Product Compliance Eng.*, Toronto, ON, Canada, Oct. 2009, pp. 1–6.

[3] R. Campbell, "Home electrical fires," NFPA Res., Quincy, MA, USA, Tech. Rep., Mar. 2019.

[4] S. H. Mortazavi, Z. Moravej, and S. M. Shahrtash, "A hybrid method for arcing faults detection in large distribution networks," *Int. J. Electr. Power Energy Syst.*, vol. 94, pp. 141–150, Jan. 2018.

[5] S. Chen, X. Li, Z. Xie, and Y. Meng, "Time–frequency distribution characteristic and model simulation of photovoltaic series arc fault with power electronic equipment," *IEEE J. Photovolt.*, vol. 9, no. 4, pp. 1128–1137, Jul. 2019.

[6] S. A. Saleh, M. E. Valdes, C. S. Mardegan, and B. Alsayid, "The state-of-the-art methods for digital detection and identification of arcing current faults," *IEEE Trans. Ind. Appl.*, vol. 55, no. 5, pp. 4536–4550, Sep. 2019.

[7] S. Lu, B. T. Phung, and D. Zhang, "A comprehensive review on DC arc faults and their diagnosis methods in photovoltaic systems," *Renew. Sustain. Energy Rev.*, vol. 89, pp. 88–98, Jun. 2018.

[8] H.-L. Dang, J. Kim, S. Kwak, and S. Choi, "Series DC arc fault detection using machine learning algorithms," *IEEE Access*, vol. 9, pp. 133346–133364, 2021.

[9] J. Jiang, W. Li, Z. Wen, Y. Bie, H. Schwarz, and C. Zhang, "Series arc fault detection based on random forest and deep neural network," *IEEE Sensors J.*, vol. 21, no. 15, pp. 17171–17179, Aug. 2021.

[10] S. Valiviita, "Zero-crossing detection of distorted line voltages using 1-b measurements," *IEEE Trans. Ind. Electron.*, vol. 46, no. 5, pp. 917–922, Oct. 1999.

[11] T. Gammon and J. Matthews, "Arcing-fault models for low-voltage power systems," in *Proc. IEEE Ind. Commercial Power Syst. Tech. Conf. Conf. Rec.*, May 2000, pp. 119–126.

[12] Y. Gao, L. Wang, Y. Zhang, and Z. Yin, "Research on AC arc fault characteristics based on the difference between adjacent current cycle," in *Proc. Prognostics Syst. Health Manag. Conf. (PHM-Qingdao)*, Oct. 2019, pp. 1–5.

[13] B. D. Russell, K. Mehta, and R. P. Chinchali, "An arcing fault detection technique using low frequency current components-performance evaluation using recorded field data," *IEEE Trans. Power Del.*, vol. PWRD-3, no. 4, pp. 1493–1500, Oct. 1988.

[14] L. Zhao, Y. Zhou, K.-L. Chen, S.-H. Rau, and W.-J. Lee, "High-speed arcing fault detection: Using the light spectrum," *IEEE Ind. Appl. Mag.*, vol. 26, no. 3, pp. 29–36, May 2020.

[15] G. Bao, R. Jiang, and X. Gao, "Novel series arc fault detector using high-frequency coupling analysis and multi-indicator algorithm," *IEEE Access*, vol. 7, pp. 92161–92170, 2019.

[16] G. Bao, R. Jiang, and D. Liu, "Research on series arc fault detection based on higher-order cumulants," *IEEE Access*, vol. 7, pp. 4586–4597, 2019.

[17] R. Jiang, G. Bao, Q. Hong, and C. D. Booth, "A coupling method for identifying arc faults based on short-observation-window SVDR," *IEEE Trans. Instrum. Meas.*, vol. 70, pp. 1–10, 2021.

[18] C. J. Kim, "Electromagnetic radiation behavior of low-voltage arcing fault," *IEEE Trans. Power Del.*, vol. 24, no. 1, pp. 416–423, Jan. 2009.

[19] A. Mukherjee, A. Routray, and A. K. Samanta, "Method for online detection of arcing in low-voltage distribution systems," *IEEE Trans. Power Del.*, vol. 32, no. 3, pp. 1244–1252, Jun. 2017.

[20] S. Zhao, Y. Wang, F. Niu, C. Zhu, Y. Xu, and K. Li, "A series DC arc fault detection method based on steady pattern of high-frequency electromagnetic radiation," *IEEE Trans. Plasma Sci.*, vol. 47, no. 9, pp. 4370–4377, Sep. 2019.

[21] Q. Xiong, S. Ji, X. Liu, X. Li, L. Zhu, X. Feng, A. L. Gattozzi, and R. E. Hebner, "Electromagnetic radiation characteristics of series DC arc fault and its determining factors," *IEEE Trans. Plasma Sci.*, vol. 46, no. 11, pp. 4028–4036, Nov. 2018.

[22] Q. Lu, Z. Ye, M. Su, Y. Li, Y. Sun, and H. Huang, "A DC series arc fault detection method using line current and supply voltage," *IEEE Access*, vol. 8, pp. 10134–10146, 2020.

[23] M. Ahmadi, H. Samet, and T. Ghanbari, "A new method for detecting series arc fault in photovoltaic systems based on the blind-source separation," *IEEE Trans. Ind. Electron.*, vol. 67, no. 6, pp. 5041–5049, Jun. 2020.

[24] N. Qu, J. Wang, and J. Liu, "An arc fault detection method based on current amplitude spectrum and sparse representation," *IEEE Trans. Instrum. Meas.*, vol. 68, no. 10, pp. 3785–3792, Oct. 2019.

[25] X. Yao, L. Herrera, S. Ji, K. Zou, and J. Wang, "Characteristic study and time-domain discrete-wavelet-transform based hybrid detection of series DC arc faults," *IEEE Trans. Power Electron.*, vol. 29, no. 6, pp. 3103–3115, Jun. 2014.

[26] H.-P. Park and S. Chae, "DC series arc fault detection algorithm for distributed energy resources using arc fault impedance modeling," *IEEE Access*, vol. 8, pp. 179039–179046, 2020.

[27] M. Ahmadi, H. Samet, and T. Ghanbari, "Series arc fault detection in photovoltaic systems based on Signal-to-Noise ratio characteristics using cross-correlation function," *IEEE Trans. Ind. Informat.*, vol. 16, no. 5, pp. 3198–3209, May 2020.

[28] R. D. Telford, S. Galloway, B. Stephen, and I. Elders, "Diagnosis of series DC Arc faults—A machine learning approach," *IEEE Trans. Ind. Informat.*, vol. 13, no. 4, pp. 1598–1609, Aug. 2017.

[29] V. Le, X. Yao, C. Miller, and B.-H. Tsao, "Series DC arc fault detection based on ensemble machine learning," *IEEE Trans. Power Electron.*, vol. 35, no. 8, pp. 7826–7839, Aug. 2020.

[30] X. Cai and R.-J. Wai, "Intelligent DC arc-fault detection of solar PV power generation system via optimized VMD-based signal processing and PSO–SVM classifier," *IEEE J. Photovolt.*, vol. 12, no. 4, pp. 1058–1077, Jul. 2022.

[31] J. Huang, X. Hu, and F. Yang, "Support vector machine with genetic algorithm for machinery fault diagnosis of high voltage circuit breaker," *Measurement*, vol. 44, no. 6, pp. 1018–1027, Jul. 2011.

[32] *UL Standard for Arc-Fault Circuit-Interrupters*, Standard UL 1699, 2008.

[33] *GB/T Standard for Arc-Fault Detection Devices*, Standard GB/T 31143, 2014.

[34] Y.-L. Shen and R.-J. Wai, "Fast-Fourier-transform enhanced progressive singular-value-decomposition algorithm in double diagnostic window frame for weak arc fault detection," *IEEE Access*, vol. 10, pp. 39752–39768, 2022.

[35] Y.-L. Shen and R.-J. Wai, "Wavelet-analysis-based singular-value-decomposition algorithm for weak arc fault detection via current amplitude normalization," *IEEE Access*, vol. 9, pp. 71535–71552, 2021.

[36] H. Lala and S. Karmakar, "Detection and experimental validation of high impedance arc fault in distribution system using empirical mode decomposition," *IEEE Syst. J.*, vol. 14, no. 3, pp. 3494–3505, Sep. 2020.

[37] W. Miao, Q. Xu, K. H. Lam, P. W. T. Pong, and H. V. Poor, "DC arc-fault detection based on empirical mode decomposition of arc signatures and support vector machine," *IEEE Sensors J.*, vol. 21, no. 5, pp. 7024–7033, Mar. 2021.

[38] N. E. Huang, Z. Shen, S. R. Long, M. C. Wu, H. H. Shih, Q. Zheng, N.-C. Yen, C. C. Tung, and H. H. Liu, "The empirical mode decomposition and the Hilbert spectrum for nonlinear and non-stationary time series analysis," *Proc. Roy. Soc. London A, Math., Phys. Eng. Sci.*, vol. 454, no. 1971, pp. 903–995, Mar. 1998.

[39] J. Su and Z. Xu, "Multi-variable method for arc-fault diagnosis based on EMD and PNN," *Electr. Power Autom. Equip.*, vol. 39, no. 4, pp. 106–113, Apr. 2019.

[40] D. P. Mandic, N. U. Rehman, Z. Wu, and N. E. Huang, "Empirical mode decomposition-based time-frequency analysis of multivariate signals: The power of adaptive data analysis," *IEEE Signal Process. Mag.*, vol. 30, no. 6, pp. 74–86, Nov. 2013.

[41] Z. Feng, D. Zhang, and M. J. Zuo, "Adaptive mode decomposition methods and their applications in signal analysis for machinery fault diagnosis: A review with examples," *IEEE Access*, vol. 5, pp. 24301–24331, 2017.

[42] J. Gilles, "Empirical wavelet transform," *IEEE Trans. Signal Process.*, vol. 61, no. 16, pp. 3999–4010, Aug. 2013.

[43] B. Xue, H. Hong, S. Zhou, G. Chen, Y. Li, Z. Wang, and X. Zhu, "Morphological filtering enhanced empirical wavelet transform for mode decomposition," *IEEE Access*, vol. 7, pp. 14283–14293, 2019.

[44] W. Gao and R.-J. Wai, "Series arc fault detection of grid-connected PV system via SVD denoising and IEWT-TWSVM," *IEEE J. Photovolt.*, vol. 11, no. 6, pp. 1493–1510, Nov. 2021.

[45] Z. Zhou and H. Xu, "A novel mean-field-game-type optimal control for very large-scale multiagent systems," *IEEE Trans. Cybern.*, vol. 52, no. 6, pp. 5197–5208, Jun. 2022.

[46] Y. Song, X. Cai, X. Zhou, B. Zhang, H. Chen, Y. Li, W. Deng, and W. Deng, "Dynamic hybrid mechanism-based differential evolution algorithm and its application," *Expert Syst. Appl.*, vol. 213, pp. 1–15, Mar. 2023.

[47] D. Wu and C. Wu, "Research on the time-dependent split delivery green vehicle routing problem for fresh agricultural products with multiple time windows," *Agriculture*, vol. 12, no. 6, p. 793, May 2022.
[48] H. Chen, F. Miao, Y. Chen, Y. Xiong, and T. Chen, "A hyperspectral image classification method using multifeature vectors and optimized KELM," *IEEE J. Sel. Topics Appl. Earth Observ. Remote Sens.*, vol. 14, pp. 2781–2795, 2021.
[49] L. Xing, Y. Wen, S. Xiao, D. Zhang, and J. Zhang, "A deep learning approach for series DC arc fault diagnosing and real-time circuit behavior predicting," *IEEE Trans. Electromagn. Compat.*, vol. 64, no. 2, pp. 569–579, Apr. 2022.
[50] H.-L. Dang, S. Kwak, and S. Choi, "Parallel DC arc failure detecting methods based on artificial intelligent techniques," *IEEE Access*, vol. 10, pp. 26058–26067, 2022.

YU-LONG SHEN received the B.S. degree in mathematical and biological sciences from the University of Alberta, Canada, in 2016, and the M.S. degree in electronic engineering from the National Taiwan University of Science and Technology, Taipei, Taiwan, in 2021. He is currently working as an Engineer at Fujian Yongfu Lvneng Technology Company Ltd., Fuzhou, Fujian, China. His research interests include machine learning and fault diagnosis.

ZHIHONG XU (Member, IEEE) was born in Linfen, Shanxi, China, in 1963. She received the B.S., M.S., and Ph.D. degrees in electronic engineering from Fuzhou University, Fuzhou, Fujian, China, in 1983, 1998, and 2006, respectively.

Since August 1983, she has been working at Fuzhou University, where she has been the Dean of the College of Electrical Engineering and Automation, since June 2016. She was elected as a Professor, in 2006. She is currently a Doctoral Supervisor and a Second-Tier Professor, the President of the Fujian Provincial Association of Women Science and Technology Workers, the Director of China Women's Association for Science and Technology, the Vice President of Fujian Provincial Electrical Engineering Society, the Director of the Fujian University Engineering Research Center for Intelligent New Energy Generation and Distribution, the Director of the Fujian Provincial Key Laboratory of Electric Energy Conversion, and the Director of the Intelligent Switch Appliance R&D Center of Fuzhou University-Xiamen Hongfa Acoustic Company Ltd. She has authored more than 200 international conferences and journal articles, including more than 60 SCI or EI papers and has been authorized with over 50 national inventive patents. She is in charge of over 40 research projects in cooperation with enterprises. The commercial applications of the projects are mostly conducted by four enterprises and have generated over 500 million yuan of direct economic value thus far. She is the author of the book *Electrical Theoretical Basis*. The first edition was published by China Machine Press, in 2014, and it is selected to be the textbook for the course of the same name by universities, including Fuzhou University, Harbin Institute of Technology, and Xi'an Jiaotong University. Her research interests include electronic products, electrical power, electronics, energy technology, and control theory applications. The outstanding achievement of her research is mainly in the area of intelligent switchgear.

Dr. Xu received the Baogang Excellent Teacher Award, in 2016, and the Lu Jiaxi Excellent Mentor Award, in 2015. She was also honored as the Leading Talent of Science and Technology Innovation of Fujian Province, in 2017. The course went online, in 2015, and was awarded National Excellent Online Course by the Ministry of Education of China, in 2017. In addition, her research "Low-voltage switch intelligent design and control technology" won the 8th Zijin Science and Technology Innovation Award of Fujian Province, in 2016, "AC contactor intelligent control and key technology of anti-voltage drop" won the second prize of Fujian Province's 2015 Science and Technology Progress Award, and "Electromagnetic System Simulation Optimized Design Platform" won the second prize of Fujian Province's 2014 Science and Technology Progress Award. Four of her team projects, including two of her personal projects, are funded by the National Natural Science Foundation of China.